Journal of Marine Science and Application (2019) 18:353–365
https://doi.org/10.1007/s11804-019-00094-6

RESEARCH ARTICLE

# Response Characteristics of Flexible Risers in Offshore Compressed Air Energy Storage Systems

Bo Hu[1] · Zhiwen Wang[1,2] · Hongwang Du[1] · Rupp Carriveau[2] · David S. K. Ting[2] · Wei Xiong[1] · Zuwen Wang[1]

Received: 8 May 2018 / Accepted: 21 February 2019 / Published online: 1 August 2019


**Abstract**
With the rapid development of marine renewable energy technologies, the demand to mitigate the fluctuation of variable generators with energy storage technologies continues to increase. Offshore compressed air energy storage (OCAES) is a novel flexible-scale energy storage technology that is suitable for marine renewable energy storage in coastal cities, islands, offshore platforms, and offshore renewable energy farms. For deep-water applications, a marine riser is necessary for connecting floating platforms and subsea systems. Thus, the response characteristics of marine risers are of great importance for the stability and safety of the entire OCAES system. In this study, numerical models of two kinds of flexible risers, namely, catenary riser and lazy wave riser, are established in OrcaFlex software. The static and dynamic characteristics of the catenary and the lazy wave risers are analyzed under different environment conditions and internal pressure levels. A sensitivity analysis of the main parameters affecting the lazy wave riser is also conducted. Results show that the structure of the lazy wave riser is more complex than the catenary riser; nevertheless, the former presents better response performance.

**Keywords** Offshore compressed air energy storage · Flexible riser · Marine energy · Catenary · Lazy wave · Sensitivity analysis

## 1 Introduction

Driven by changing climate, evolving energy demand, and favorable economics, the renewable proportions of energy portfolios are growing rapidly. They are also increasingly integrated with storage technologies that enhance their flexibility. The ocean, accounting for 71% of the planet, contains enormous unexploited renewable energy resources (Bahaj 2011; Stegman et al. 2017).

In recent years, marine renewable energy has drawn increasing interest as marine renewable energy technologies continue to mature. The UK, which is considered a global leader in this field, proposed the Marine Energy Action Plan early in 2010 (Government 2010). Soon after, the European Commission, the Mid-Atlantic Regional Planning Body, and China released plans to develop marine renewable energy (European Commission 2014; Mid-Atlantic Regional Planning Body 2016).

Marine renewable energy covers many forms, such as offshore wind, offshore solar, wave, tide, current, temperature, and salinity gradient (Bahaj 2011). Similar to their terrestrial counterparts, most marine renewable energy sources are unsteady, intermittent, stochastic, and far from the end users; these limitations can cause power stability as well as transmission, energy, and economic challenges (Zhou et al. 2016). Energy storage is one of the most promising options for resolving these issues (Zhou et al. 2013; Liu and Zhang 2016; Tang et al. 2017; Wang et al. 2017). However, the challenge of a harsh marine environment and difficult business cases has restricted the widespread commercial success of marine renewable energy storage. Beyond infantile battery energy

**Article Highlights**
- The response characteristics of gas conveying risers in an offshore compressed air energy storage system are analyzed for the first time.
- The response characteristics of flexible riser under different environmental conditions and internal gas pressure are analyzed in OrcaFlex.
- The lazy wave riser presents better response performance when compared with catenary riser under the same environmental conditions.
- The effective tension and bending curvature of lazy wave riser are sensitive to position, length, and size of the buoyancy module.

✉ Wei Xiong
xiongwei@dlmu.edu.cn

[1] Institute of Ship Electromechanical Equipment, Dalian Maritime University, Dalian 116026, China

[2] Turbulence and Energy Laboratory, Ed Lumley Centre for Engineering Innovation, University of Windsor, Windsor, Ontario N9B 3P4, Canada

storage, other novel marine renewable energy storage technologies have emerged; such technologies include offshore compressed air energy storage (OCAES), offshore pumped hydro energy storage, offshore hydrogen energy storage, offshore gravity energy storage, and buoyancy energy storage (Komor and Glassmaire 2012; Lim et al. 2013; Slocum et al. 2013; Pimm et al. 2014; Lan et al. 2015; Li and Decarolis 2015; Serna et al. 2016; Vasel-Be-Hagh et al. 2015; Wang et al. 2016; Zanuttigh et al. 2016; Bassett et al. 2016; Hahn et al. 2017; Germa and MGH-deep sea storage 2010). Many of these energy storage technologies offer promise to create integrated, dispatchable energy systems based on the great resource potential of the sea.

Among the aforementioned marine renewable energy storage technologies, OCAES is the most developed and regarded as a flexible-scale energy storage technology. The world's first utility-scale OCAES system was established and activated by Hydrostor Corp. in 2015 (Hydrostor Corp 2015). IRWA (International Renewable Energy Agency) and DNV&GL (Det Norske Veritas and Germanischer Lloyd) predict that the large-scale deep-water offshore wind farm and offshore energy storage systems will be commercially deployed before 2050; they also highlighted the particular critical role of future OCAES technology (DNV 2014; Abu Dhabi 2016). Compared with onshore CAES, the underwater subsystem is unique to OCAES, where risers are required to transport compressed air into and out of deep-water air accumulators. Despite examples of OCAES research and commercial activity, few studies are available regarding the viability of risers in OCAES systems.

Marine risers are critical components of offshore applications in ocean engineering because they provide a means of transferring fluids or power between subsea units and a top-side floating platform or buoys (Hoffman et al. 1991; Institution 2006; Zhu and Gao 2017; Zhu et al. 2017). According to their structures and functions, marine risers can be divided into four categories: top tension riser, steel catenary riser, flexible riser, and hybrid riser (Lshii et al. 1995; Cuamatzi-Melendez et al. 2017). In deep-water applications, flexible risers can suffer large displacements because bending stiffness is lower than axial and torsional stiffness. These risers require special nonlinear analysis (Kordkheili and Bahai 2007; Pham et al. 2016; Santillan and Virgin 2011). Flexible risers are an enabler for deep-water (< 1000 m) and ultra-deep-water (> 1000 m) developments for over 26 years in marine oil and gas production systems (Hill et al. 2006; Wang and Duan

**Table 1** Actual system parameters

| Parameter type | Value |
|---|---|
| Water depth (m) | 500 |
| Inner diameter of riser (m) | 0.250 |
| Pressure of compressed air (MPa) | 5.1 |

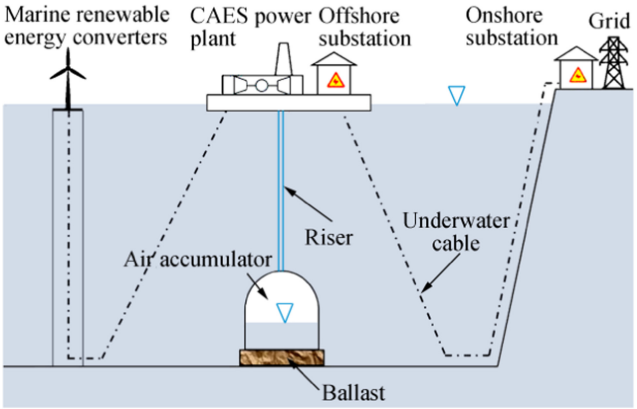


**Fig. 1** Typical configuration of an OCAES system

2015). Thus far, the deepest application of a flexible riser is 2438.4 m. The riser diameter ranges from 50.8 to 482.6 mm. The maximum design pressure can reach 103.4 MPa, and the maximum operating temperature can reach 130 °C (Yu et al. 2014). At present, spatial discrete methods for the physical and mechanical models of flexible risers are categorized into three kinds, namely, concentrated mass method, finite difference method, and finite element method (FEM). The concentrated mass method is based on the physical model of the flexible riser, which is regarded as a series of massless springs connected to discrete concentrated mass nodes. Ghadimi and Boom et al. first obtained the bending moment by the change in each slope and calculated the equivalent shear force (Ghadimi 1988; Boom et al. 1987). Raman-Nair and Baddour deduced the generalized active force of the spring in the local coordinate system, but the author used the Kane equation to describe the control equation; as such, the derivation process was very complex, which greatly reduces the simulation efficiency of the concentrated mass method (Raman and Baddour 2003). This method can be used to analyze the dynamic response of the variable length towing cable system; the main advantage is that it is easy to simulate the process of release and recovery with high efficiency (Kamman and Huston 2001). Miao used a quasi-steady time domain method to analyze the motion and dynamic characteristics of a mooring system under the combined action of wind, wave, and flow; the dynamic characteristics of the anchorage chain were obtained by a generalized mass method (Miao 1998). Zhu adopted the model and proposed a method for time domain analysis of the three-dimensional dynamic performance of an ocean cable integrated system (Zhu et al. 2002). Compared with the concentrated mass method, the finite difference method is more based on differential equations in mathematics. However, this method is not easy to deal with due to the boundary conditions and existence of a convergence problem. Jain used a finite difference scheme for static analysis of the lazy-S riser drape section (Jain 1994). Jason derived the two-dimensional motion equation of underwater cable considering bending stiffness in the geometric

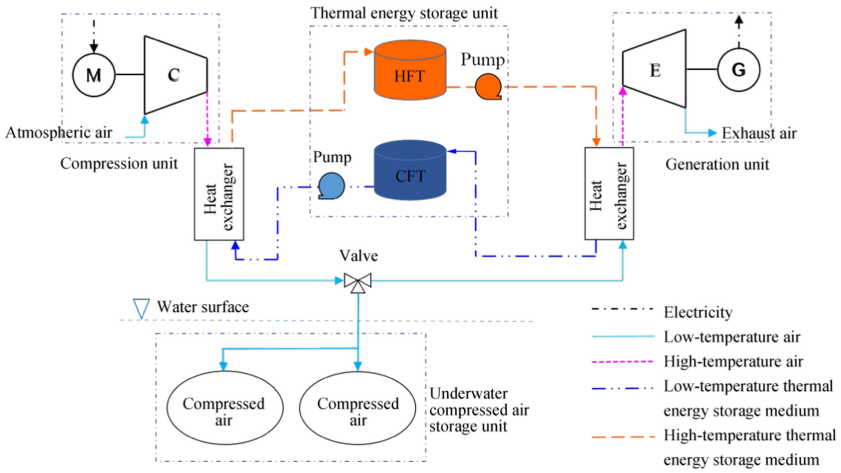


**Fig. 2 An OCAES power plant.** C compressor, E expander, G generator, M motor, HFT hot thermal energy storage fluid tank, CFT cold thermal energy storage fluid tank

compliance mooring system; the equation was discrete in the space domain by a box method and integrated with the generalized alpha method in the time domain (Gobat 2000). Santillan used elastic line theory to analyze the large deformation problem and employed shooting and finite difference methods for numerical solution; finally, an example of a steep riser was given (Santillan 2007). The FEM is based on the elastic mechanics and can discrete the cable into a finite element. Xie and Gao introduced two-dimensional finite element analysis of the dynamic characteristics of an integrated ocean cable system composed of surface buoys, cables, and intermediate objects (Xie and Gao 2000). Long and Tan established the dynamic response of the mooring system in the time domain by establishing the FEM of the contact line between the mooring line and the seabed under marine environment load (Long and Tan 2005). Yuan et al. used the FEM in the time domain to establish a numerical model of the cable equation, taking the simulation comparison of the single mooring and multi-point mooring as examples; they also developed the corresponding calculation program (Yuan et al. 2010a, b). At present, flexible risers are mainly used to convey liquid or gas–liquid mixtures. Our literature survey indicated a dearth of research on flexible marine risers conveying single-phase high-pressure gas. The prolific flexible riser technology in the oil and gas industry will provide a valuable reference for research on developing flexible risers in OCAES systems.

In this study, the response characteristics of flexible risers in OCAES systems are investigated for the first time. Two

**Table 2** Riser data sheet unit: mm

| Layer No. | Description | Material | Inner diameter | Thickness | Outer diameter |
|---|---|---|---|---|---|
| 1 | Carcass layer | Carbon steel | 250 | 7 | 264 |
| 2 | Internal pressure sheath | PVDF | 264 | 4 | 272 |
| 3 | Internal pressure sheath | PVDF | 272 | 12 | 296 |
| 4 | Pressure armor | Steel | 296 | 12 | 320 |
| 5 | Antiwear | PALL | 320 | 1.5 | 323 |
| 6 | 1st tensile armor layer | Steel | 323 | 6 | 335 |
| 7 | Antiwear | PALL | 335 | 0.4 | 335.8 |
| 8 | Antiwear | PALL | 335.8 | 1.5 | 338.8 |
| 9 | 2nd tensile armor layer | Steel | 338.8 | 6 | 350.8 |
| 10 | Antiwear | PALL | 350.8 | 0.4 | 351.6 |
| 11 | Antiwear | PALL | 351.6 | 1.5 | 354.6 |
| 12 | 3rd tensile armor layer | Steel | 354.6 | 6 | 366.6 |
| 13 | Antiwear | PALL | 366.6 | 0.4 | 367.4 |
| 14 | Antiwear | PALL | 367.4 | 1.5 | 370.4 |
| 15 | 4th tensile armor layer | Steel | 370.4 | 6 | 382.4 |
| 16 | Antiwear | PALL | 382.4 | 0.4 | 383.2 |
| 17 | Antiwear | PALL | 383.2 | 0.4 | 384 |
| 18 | Outer sheath | PVDF | 384 | 12 | 408 |

**Table 3** Structure parameters of the flexible riser

| Parameter type | Value |
|---|---|
| Length of catenary riser (m) | 960 |
| Length of lazy wave riser (m) | 780 |
| Outer diameter (m) | 0.408 |
| Inner diameter (m) | 0.250 |
| Mass per unit length (kg/m) | 404 |
| Bending stiffness (kN · $m^2$) | 203 |
| Axial stiffness (kN) | 3.8E6 |

options, namely, catenary riser and lazy wave riser, are analyzed. According to the actual system parameters shown in Table 1, the flexible risers are designed and analyzed numerically. Static and dynamic analyses are performed, and the results are compared. The main factors of the buoyancy module that influence the global response characteristic of the system are also analyzed by simulations.

The paper is organized as follows. In Section 2, the system configuration and working processes of the OCAES system are introduced. The numerical models of the catenary riser and the lazy wave riser are established in Section 3. In Section 4, the effective tension and the shape of the flexible riser in the static and dynamic models are analyzed. A sensitivity analysis is also conducted for the main parameters of the buoyancy module. Finally, conclusions are drawn.

## 2 Offshore Compressed Air Energy Storage System

A typical OCAES system is shown in Fig. 1. Electricity is generated by the marine renewable energy converters (MREC), collected, and transformed in the offshore substation. Surplus (because of low demand/low market price)

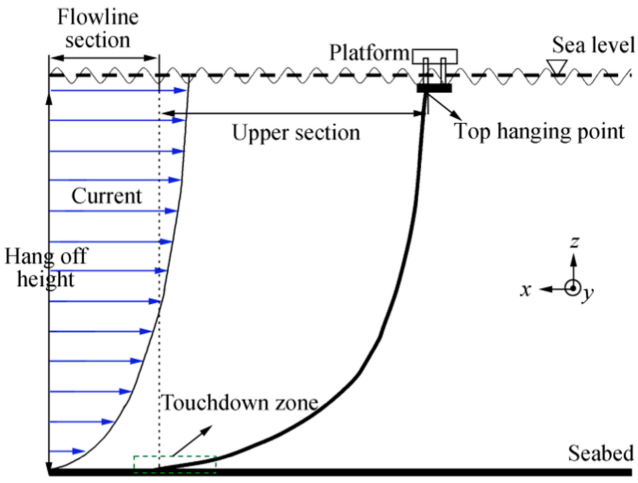


**Fig. 3** Model of the catenary riser

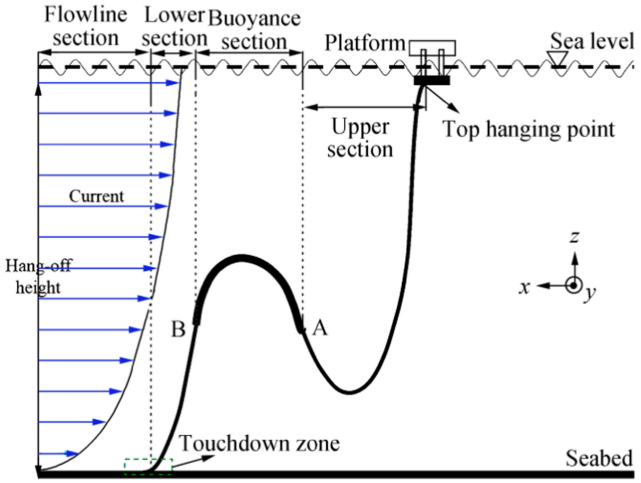


**Fig. 4** Model of the lazy wave riser

electricity from the MREC is used to charge the CAES power plant. In the CAES power plant, electricity energy is converted into thermal and pressure energy carried in compressed air. The high-pressure compressed air is transported into air accumulators, which are ballasted to the seabed. When needed, the stored compressed air is released from the air accumulators to drive turbo expanders, which regenerate electricity. This electricity is transmitted to the onshore substation and grids via underwater cables. Thus, this energy storage system can be realigned for offshore oil and gas platforms, islands, and coastal cities, where available topography exists.

Figure 2 shows a simplified schematic of an OCAES power plant.

The system can be divided into compressed air storage and thermal energy storage subsystems, which are connected via heat exchangers. The compressed air storage subsystem is primarily used to store compressed air. Excess electricity drives the electric motor (M). Atmospheric air is drawn into and compressed in the air compressor (C). After cooling in the heat exchanger, the compressed air is charged into the air accumulators via the riser. When needed, the stored compressed air is discharged from the air accumulators and reheated in the heat exchanger to drive the air expander (E) and generate electricity in the generator (G). The compression unit generates a significant amount of heat, which is used to

**Table 4** Environment parameters

| Parameter type | Value |
|---|---|
| Seawater density (kg/$m^3$) | 1025 |
| Wave period (s) | 7.0 |
| Wave length (m) | 80.8 |
| Wave height (m) | 6.0 |
| Surface current (m/s) | 2.01 |
| Seabed current (m/s) | 0 |

**Table 5** Boundary conditions

| Catenary riser | | Lazy wave riser | |
|---|---|---|---|
| Top hanging point | (36, 1.7, − 7.5) | Top hanging point | (36, 1.7, − 7.5) |
| Touchdown zone | (600, − 35, 0.2) | Touchdown zone | (420, − 35, 0.2) |
| Hanging angle | 20° | Hanging angle | 15° |

heat up the working fluid from the cold thermal energy storage tank and is stored in the hot thermal energy storage tank. In the discharging stage, the stored thermal energy in the hot thermal energy storage fluid tank (HFT) is utilized to heat the cold air via the heat exchanger on the expansion site, before returning to the cold compressed air. In this way, the thermal energy generated in compression is not wasted.

## 3 System Modeling of a Flexible Riser System

Based on the pressure condition of the OCAES system, flexible riser parameters are designed using the API Recommended Practice 17B (API 2008). The riser data sheet is presented in Table 2. Although the structure of the flexible riser is very complex, it can be assumed as a homogeneous pipeline for simplification. The equivalent structural parameters of the flexible riser are shown in Table 3.

The numerical model of the catenary riser and the lazy wave riser is established in OrcaFlex software (Figs. 3 and 4). The flexible riser is established by the line unit, and the buoyancy module of the lazy wave is established by the clump unit. The inside of the flexible riser is filled with high-pressure compressed air with a density of 60.5 kg/m$^3$. The top of the flexible riser is attached to the bottom of the platform, while the end of the riser is connected to the seabed by an anchored boundary condition. The friction coefficient between the soil and the riser is set as 0.5 (OrcaFlex). The environmental parameters, both wave and current, used in the calculation are shown in Table 4. The boundary conditions are shown in Table 5.

Compared with other methods, lumped mass method has many advantages (Huang and Vassalos 1993; You et al. 2008): (l) explicit physical meaning of mathematical model; (2) high efficiency for calculating the tension and riser configuration; and (3) suitability for non-linear, unsteady state, non-uniform riser and oscillation flow analyses (Fig. 5).

The motion equation of the $i$th node on the flexible riser is as follows:

$$m_i \boldsymbol{a}_i + \frac{1}{2} e_{i+1/2} \boldsymbol{a}_{iN} \Big|_{i+1/2} + \frac{1}{2} e_{i-1/2} \boldsymbol{a}_{iN} \Big|_{i-1/2} = \boldsymbol{F}_i \qquad (1)$$

where $m_i$ is the mass, $\boldsymbol{a}_i$ is the acceleration, $e_{i+1/2}$ is the imaginary masses of the fluid being dragged between nodes $i$ and $i+1$, $e_{i-1/2}$ is the imaginary masses of the fluid being dragged between nodes $i$ and $i-1$, $\boldsymbol{a}_{iN}|_{i+1/2}$ and $\boldsymbol{a}_{iN}|_{i-1/2}$ are the normal components of vector $\boldsymbol{a}_i$ on two segments, and force

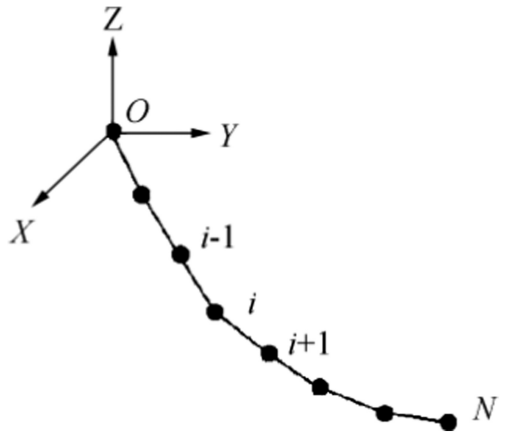


**Fig. 5** Lumped mass method model

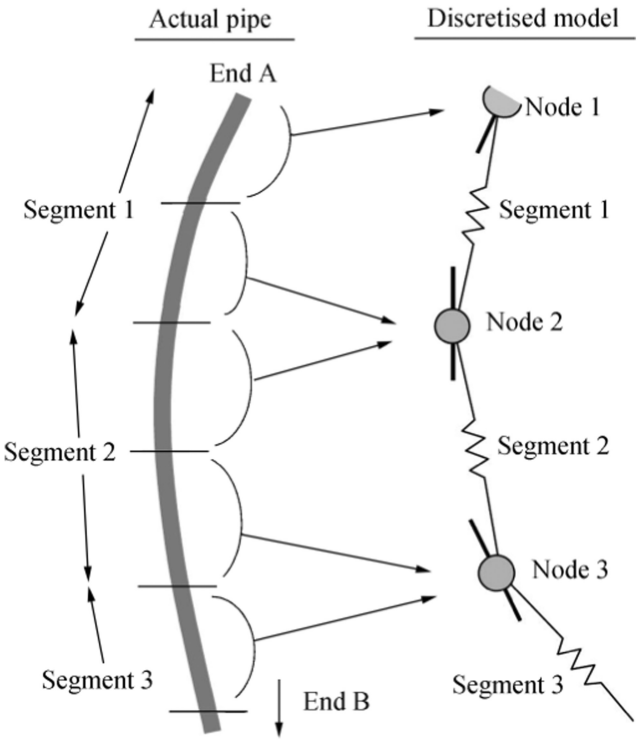


**Fig. 6** OrcaFlex line model (OrcaFlex)

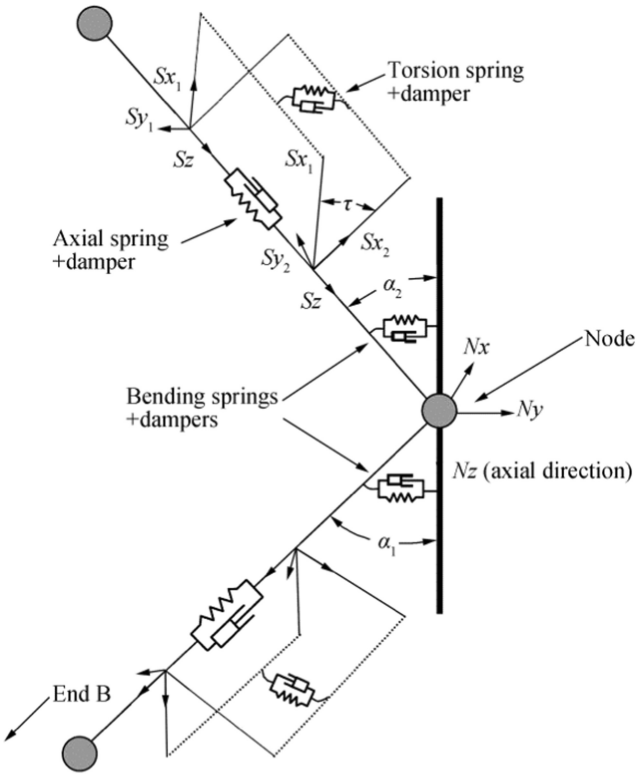


**Fig. 7** Detailed representation of the OrcaFlex line model (OrcaFlex)

vector $\boldsymbol{F}_i$ includes tension, drag force, gravity, buoyancy, and any other external forces in two segments.

The basic mechanism of dynamic tension in the riser system is inertia force, tension force, geometric stiffness, and elastic stiffness. Except for the case that the riser is tensioned or has obvious high-frequency motion, the elastic stiffness in most riser systems of compliant platforms is ignored, and the spring-mass-damping system takes into account all these physical parameters.

Figures 6 and 7 show the finite element model of the riser used in OrcaFlex (ORCAFLEX 2017). The model is based on the theory of the lumped mass method, which is commonly used for analyzing slender rod structures. The riser is divided into a series of segments, which are then modeled by a straight massless model segment with a node at each end. The model section only simulates the axial and torsional properties of the riser, while other properties (mass, weight, buoyancy, etc.) are all lumped into the nodes numbered as 1, 2, 3, etc. in Fig. 6.

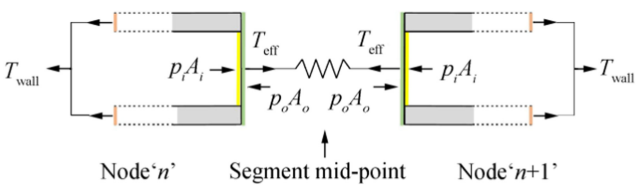


**Fig. 8** Tension and pressure force

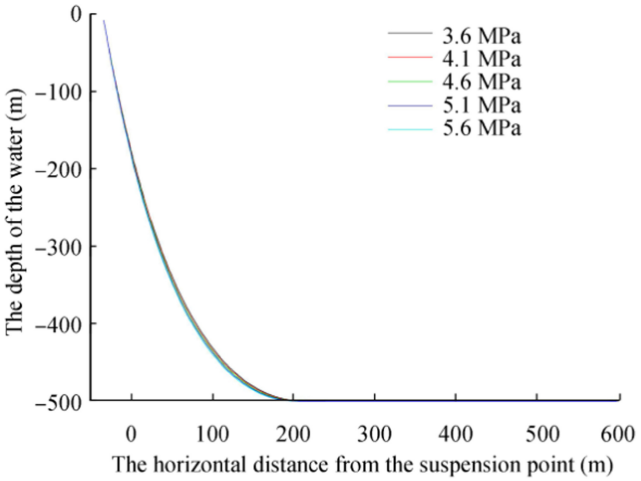


**Fig. 9** Influence of different internal pressure levels on the shape of the catenary riser

Figure 7 presents the details of the line model, showing a single mid-line node and the segments on either side of it. The figure includes the various spring and dampers that model the structural properties of the line. The three types of spring and dampers in the model are as follows:

1) The axial stiffness and damping of the line are modeled by the axial spring and damper at the center of each segment, which applies an equal and opposite effective tension force to the nodes at each end of the segment.
2) The bending properties are represented by rotational spring and dampers on either side of the node, spanning between the node's axial direction *Nz* and the segment's axial direction *Sz*.
3) The line's torsional stiffness and damping are modeled by torsional spring and damper at the center of each segment, which applies equal and opposite torque moments to the nodes at each end of the segment.

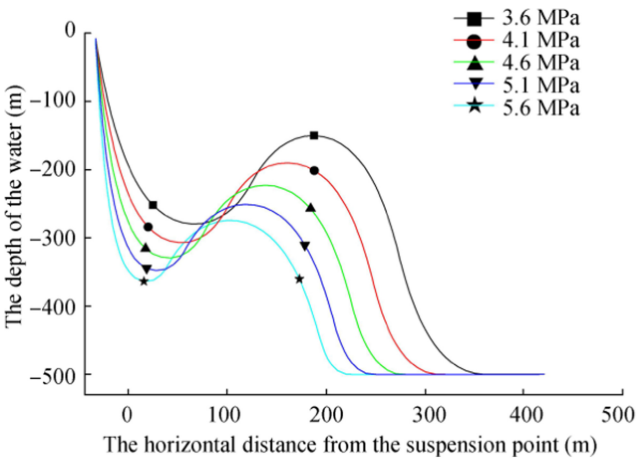


**Fig. 10** Influence of different internal pressure levels on the shape of the lazy wave riser

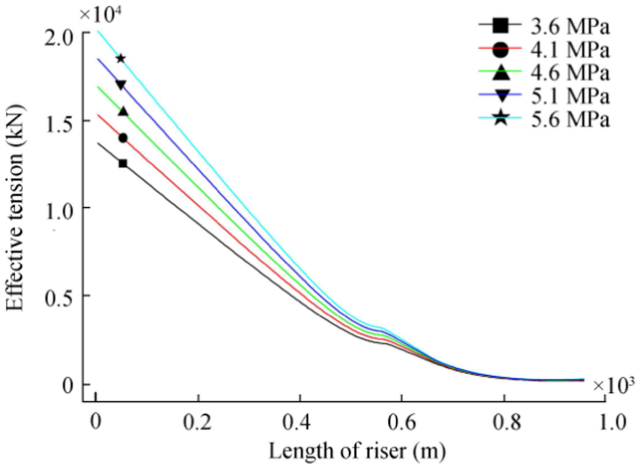


**Fig. 11** Influence of different internal pressure levels on the effective tension of the catenary riser

In OrcaFlex, the two types of tension reported are effective tension ($T_{\text{eff}}$) and wall tension ($T_{\text{wall}}$), which are related by:

$$T_{\text{eff}} = T_{\text{wall}} - p_{\text{i}}A_{\text{i}} + p_0A_0 \tag{2}$$

where $p_{\text{i}}$ is the internal pressure (pressure of compressed air), $p_0$ is the external pressure (pressure of surrounding water), and $A_{\text{i}}$ and $A_0$ are the internal and external cross section areas of the stress annulus of the riser, respectively.

The difference between the effective tension and the wall tension is shown in Fig. 8. The nodes in the two sides represent a length of riser with its contents. The forces on them are calculated as if the length of the pipe represented has end caps, which hold in the contents and are exposed to internal and external pressure. Therefore, a force balance presented by Eq. (1) is formed in the axial direction (OrcaFlex).

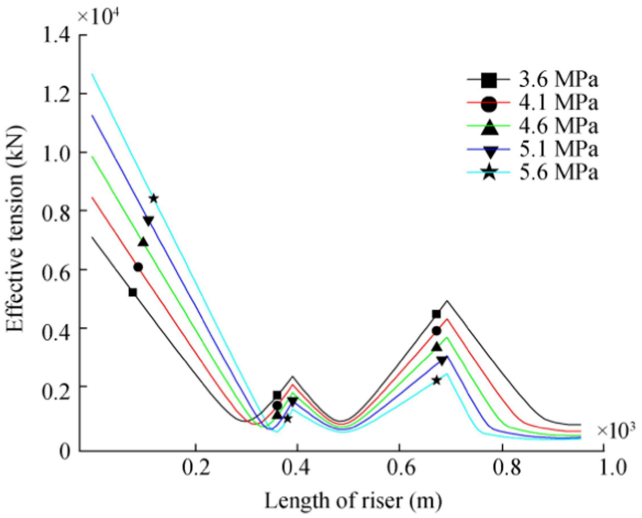


**Fig. 12** Influence of different internal pressure levels on the effective tension of the lazy wave riser

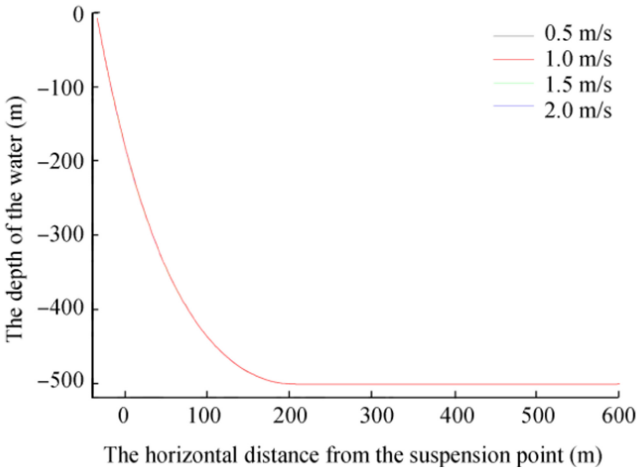


**Fig. 13** Influence of different types of current flow on the shape of the catenary riser

## 4 Global Response Analysis of the Riser System

### 4.1 Static Response Characteristics

Based on the established model, the static response characteristics of the flexible riser are analyzed first. The objective for the static analysis is to determine the equilibrium configuration of the system under weight, buoyancy, and hydrodynamic forces, thereby providing a starting configuration for the dynamic simulation. The influence of different internal pressure levels and current flow on the flexible riser is determined, and the response characteristics of the flexible riser are analyzed.

Figure 9 shows the influence of different internal pressure levels on the shape of the catenary riser in a static state. The internal pressure varies from 3.6 to 5.6 MPa. The result shows that the internal pressure of air has negligible impact on the shape of the catenary riser in the static state.

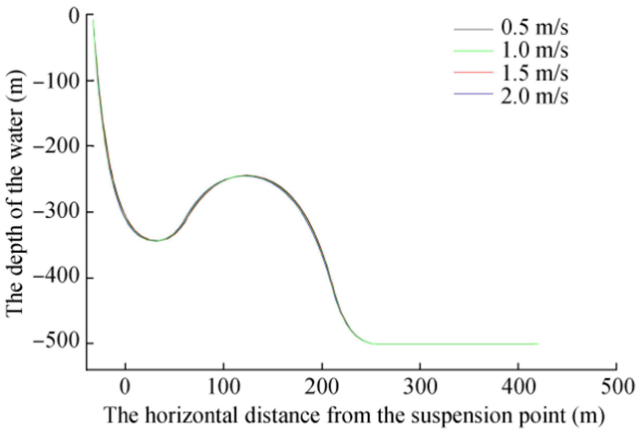


**Fig. 14** Influence of different types of current flow on the shape of the lazy wave riser

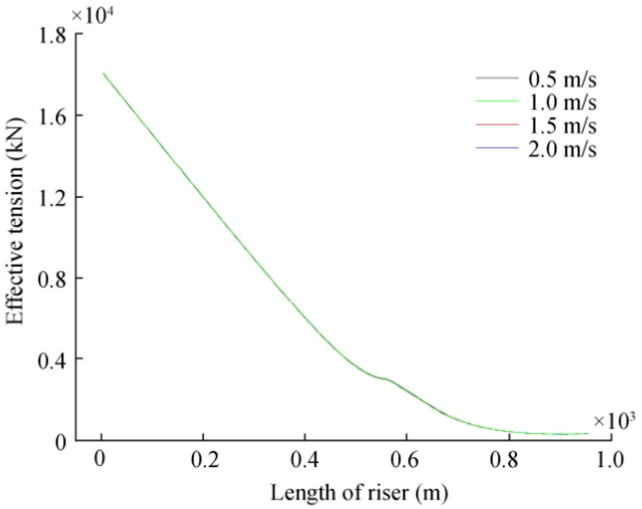


**Fig. 15** Influence of different types of current flow on the effective tension of the catenary riser

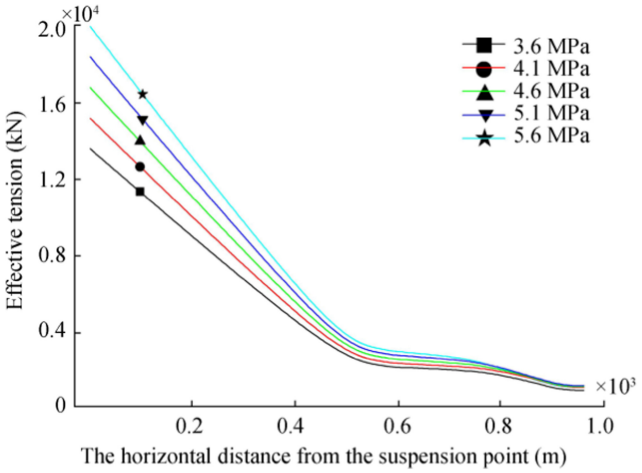


**Fig. 17** Influence of different internal pressure levels on the effective tension of the catenary riser

Figure 10 shows the influence of different internal pressure levels on the shape of the lazy wave riser in a static state. The internal pressure has a greater impact on the lazy wave riser than that on the catenary riser. The height of the float section decreases with increasing internal pressure at the buoyancy section.

Figure 11 shows the influence of different internal pressure levels on the effective tension of the catenary riser in a static state. The result shows that the effective tension on the top hanging point increases with increasing internal pressure. The influence of internal pressure decreases along the length of the riser.

Figure 12 shows the influence of different internal pressure levels on the effective tension of the lazy wave riser in a static state. The maximum effective tension of the lazy wave riser is smaller than that of the catenary riser. The result shows that the effective tension on the top hanging point increases with increasing internal pressure. Meanwhile, the effective tension on the buoyance section decreases with increasing internal pressure.

Figures 13 and 14 show the influence of different types of current flow on the shape of the catenary riser and lazy wave riser in a static state, respectively. The distribution of current flow varies from 0.5 to 2.0 m/s, and the current method is interpolated. The result shows that the current flow has negligible impact on the shape of the catenary riser and the lazy wave riser.

Figures 15 and 16 show the influence of different types of current flow on the effective tension of the catenary riser and the lazy wave riser in a static state, respectively. The result shows that the current flow has little impact on the effective tension of the catenary riser and the lazy wave riser.

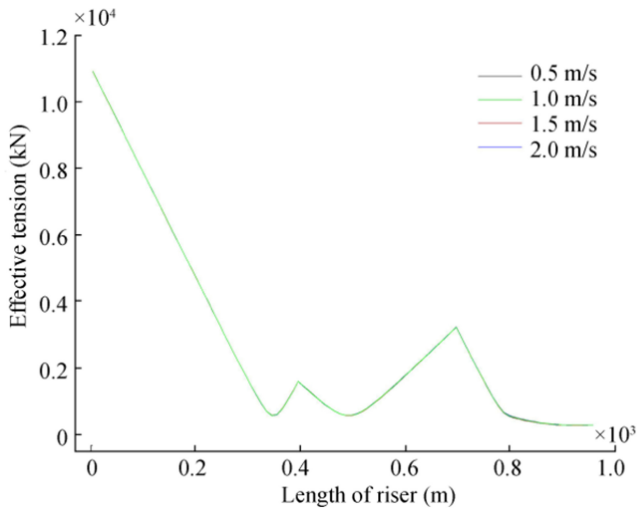


**Fig. 16** Influence of different types of current flow on the effective tension of the lazy wave riser

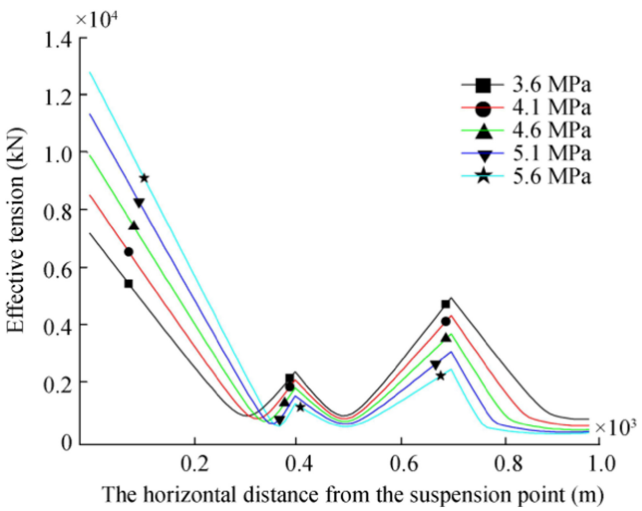


**Fig. 18** Influence of different internal pressure levels on the effective tension of the lazy wave riser

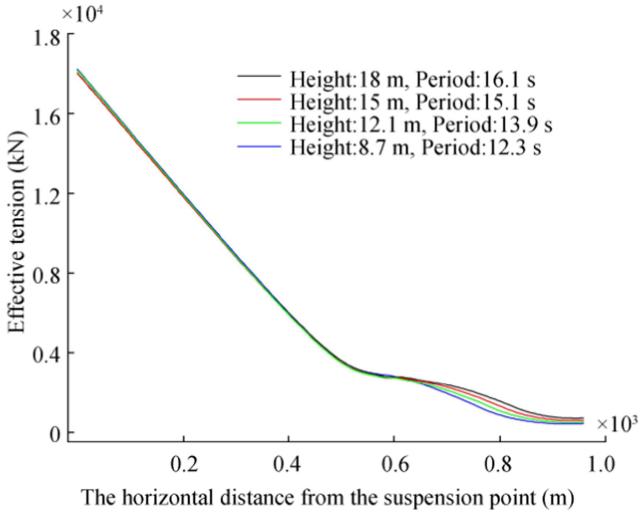


**Fig. 19** Influence of different wave conditions on the effective tension of the catenary riser

## 4.2 Dynamic Response Characteristics

The dynamic response of the two configurations of the flexible risers are calculated and compared under the same conditions. The dynamic analysis is a time simulation of the motions of the model over a specified period of time, starting from the position derived by the static analysis.

Figure 17 shows the influence of different internal pressure levels on the effective tension of the catenary riser in a dynamic state. The result shows that the effective tension on the top hanging point increases with increasing internal pressure. In addition, the influence of internal pressure decreases along the length of the riser.

Figure 18 shows the influence of different internal pressure levels on the effective tension of the lazy wave riser in a dynamic state. The result shows that the effective tension on the top hanging point increases with increasing internal pressure. By contrast, the effective tension on the buoyancy section decreases with increasing internal pressure.

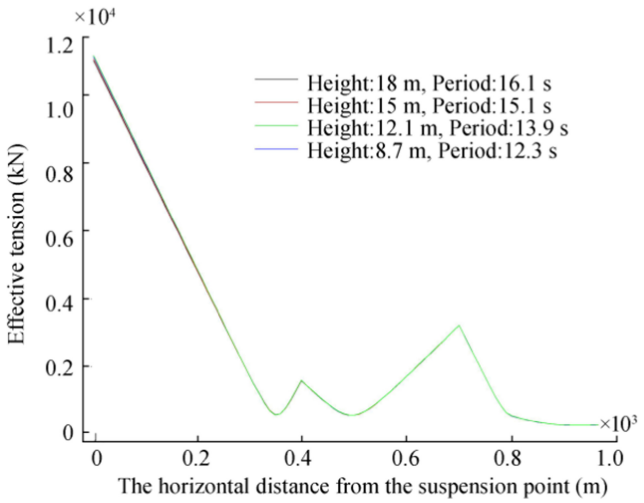


**Fig. 20** Influence of different wave conditions on the effective tension of the lazy wave riser

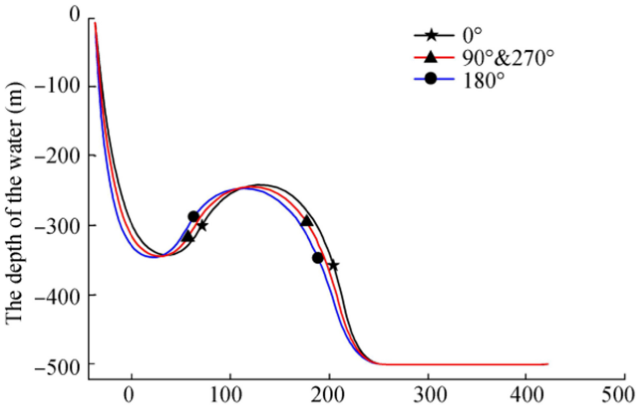


**Fig. 21** Steady state shapes of the flexible riser in different current directions

Figures 19 and 20 show the influence of different wave conditions on the effective tension of the flexible riser in a dynamic state. The height of the wave varies from 8.7 to 18 m, and the period varies from 12.3 to 16.1 s. The result shows that the wave conditions have little impact on the effective tension of the catenary riser and the lazy wave riser.

Figure 21 shows the steady state shapes of the flexible riser in different current directions. The current directions vary from 0 to 270° with 90° increments. The projected steady state shapes of the flexible riser in the *XOZ* plane are the same because of the plane symmetry of the 90° current and 270° current about the *XOZ* plane. For the dynamic analysis, the effects of different current directions on the shapes of the flexible riser are not significant; thus, only the 180° current is considered for the analysis of dynamic response characteristics.

Figures 22 and 23 show the dynamic vertical displacement at 460 m point in the two studied configurations. The

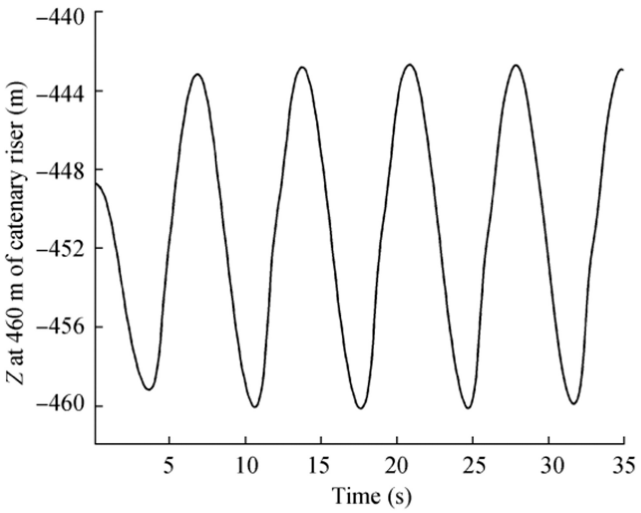


**Fig. 22** Dynamic vertical displacement of the catenary riser at 460 m point

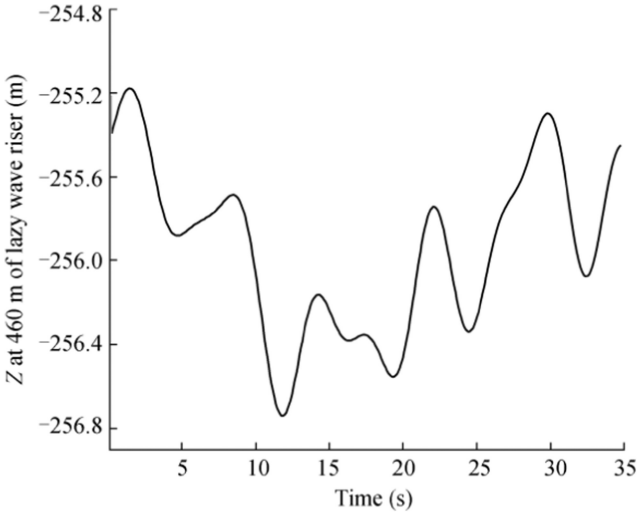


**Fig. 23** Dynamic vertical displacement of the lazy wave riser at 460 m point

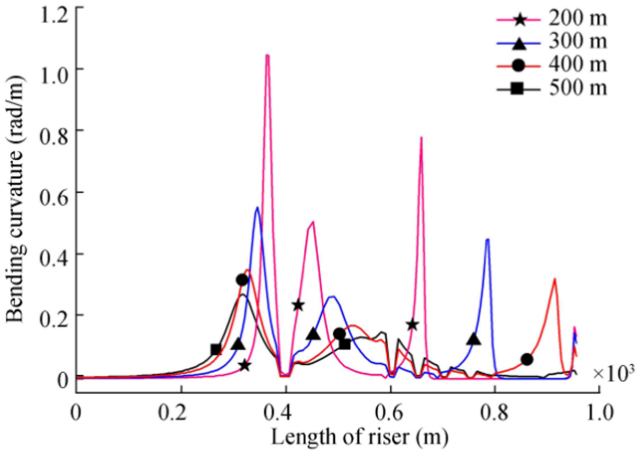


**Fig. 25** Comparison of bending curvature of different buoyancy modules with various lengths

displacement of the catenary riser is larger than that of the lazy wave riser, indicating that the lazy wave configuration performs better in terms of global displacement response.

### 4.3 Sensitivity Analysis of Lazy Wave Parameters

The parameters of the buoyancy module are the main factors that affect the global response of the lazy wave riser. Thus, a parametric sensitivity analysis of the global response of the lazy wave riser is performed.

The length of the buoyancy module is an important factor that affects the global response of the lazy wave riser. The static effective tension and the bending curvature of the lazy wave riser with 200 m, 300 m, 400 m, and 500-m buoyancy modules are analyzed. Figure 24 shows that the effective tension of the top hanging point decreases while the effective tension at the end of the buoyancy module increases with increasing buoyancy module.

Figure 25 illustrates that the local maximum values of the bending curvature of the buoyancy module decrease as the buoyancy module lengthens. As such, appropriate extension of the buoyancy module can improve the bending performance of the flexible riser.

The position of the buoyancy module can alter the waveform of the lazy wave riser. Thus, the static effective tension and the bending curvature of the lazy wave riser are analyzed in the context of the location of the buoyancy module. Specifically, the starting point of the buoyancy module is varied from 200 to 500 m in 100 m increments. Figure 26 shows that the effective tension at the top hanging point increases as the start of the buoyancy module is delayed. On the other hand, the maximum value of the effective tension increases with the starting position of the buoyancy module. Figure 27

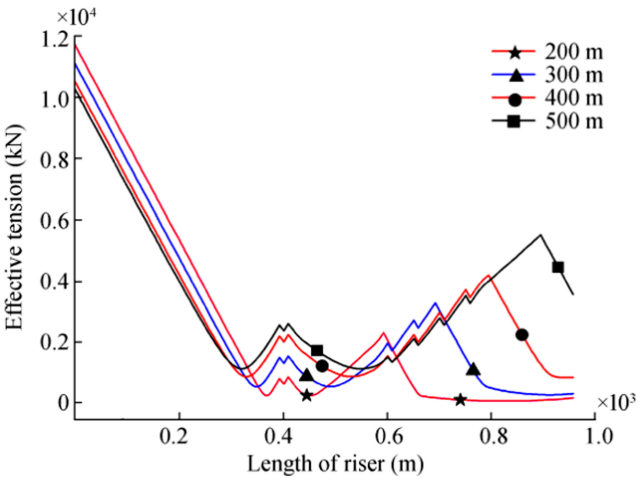


**Fig. 24** Comparison of effective tension of different buoyancy modules with various lengths

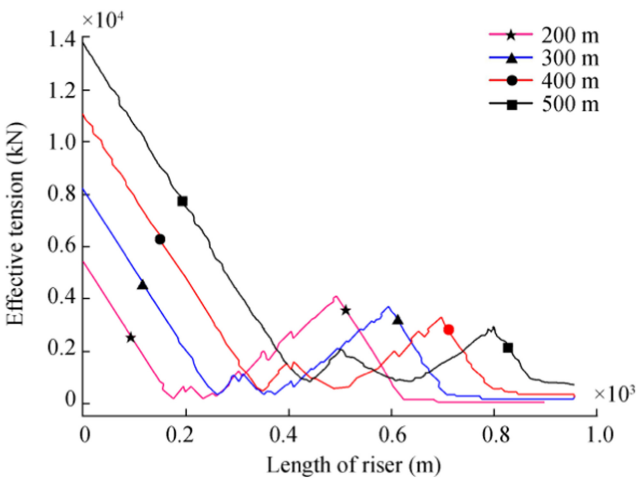


**Fig. 26** Comparison of effective tension for different positions of the buoyancy module

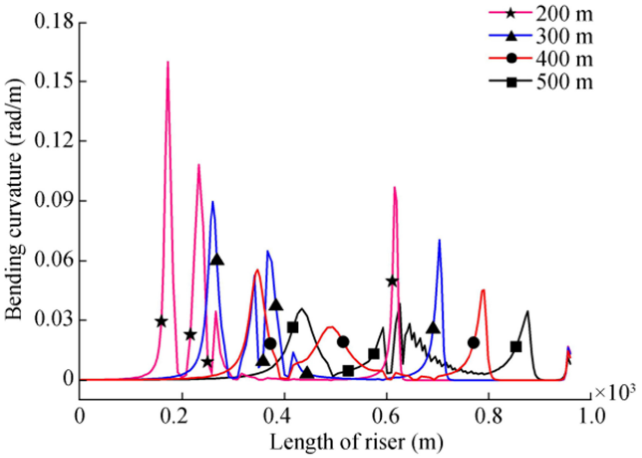


**Fig. 27** Comparison of bending curvature for different positions of the buoyancy module

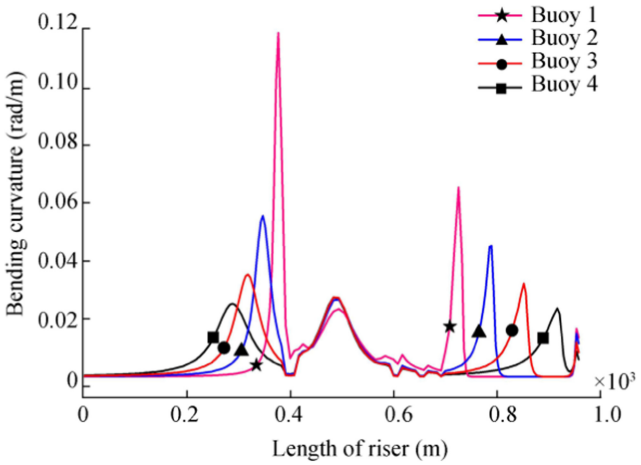


**Fig. 29** Comparison of bending curvature for different sizes of the buoyancy module

shows that the bending performance of the lazy wave flexible riser is better as the buoyancy module is postponed.

Other than the starting position, the size of the buoyancy module can provide different levels of buoyancy for the lazy wave riser. The static effective tension and the bending curvature of the lazy wave riser are analyzed in terms of the size of the buoyancy module. The size of "buoy 1" buoyancy module is the smallest, and that of "buoy 4" is the largest. The results are shown in Figs. 28 and 29. The effective tension at the top hanging point decreases with the increasing value of the buoyancy module. However, an increase in the size of the buoyancy module also increases the buoyancy, which in turn increases the effective tension in the buoyancy module. The bending curvature local maximum values of the lazy wave flexible riser decrease with the increasing size of the buoyancy module. Hence, the buoyancy module can improve the global bending performance.

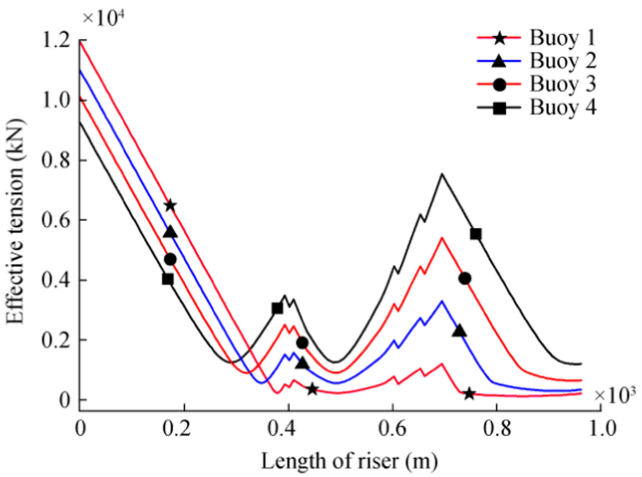


**Fig. 28** Comparison of effective tension for different sizes of the buoyancy module

## 5 Conclusions

In an effort to push deep-water OCAES technology closer to implementation, marine riser approaches from the oil and gas industry are introduced and investigated for this new application for the first time. The numerical models of two kinds of flexible risers, namely, catenary riser and lazy wave riser, are established in OrcaFlex software. The static and dynamic characteristics of the catenary and the lazy wave risers are analyzed under different environment conditions and internal pressure levels. A sensitivity analysis of the main buoyancy module parameters affecting the lazy wave riser is also conducted. The results show that the structure of the lazy wave riser is more complex than the catenary riser; nevertheless, the lazy wave riser presents better response performance. The detailed main conclusions are as follows:

1) In the static analysis, the effective tension of the catenary riser gradually decreases along its length. The lazy wave riser shows maximum values in the buoyancy module, although these maximum values are significantly smaller than those associated with the catenary riser. The effective tension of the catenary riser and the lazy wave riser is influenced by internal pressure.
2) In the dynamic analysis, the effective tension of the catenary riser is more intense than that of the lazy wave riser. This finding implies that the lazy wave riser can be utilized to improve the dynamic response of the OCAES system, i.e., stabilize the OCAES system.
3) In the sensitivity analysis, the maximum bending curvature and the effective tension at the top hanging point decrease with elongation and the enlargement of the buoyancy module. With decreasing distance between the buoyancy module and the top hanging point, the

maximum effective tension of the top hanging point increases while the maximum bending curvature decreases. Therefore, a balance between these parameters is required.

**Funding** This work was supported by the Fundamental Research Funds for the Central Universities of China (grant numbers 3132016353, 3132019117, 3132019122) and the Natural Sciences and Engineering Research Council of Canada.

## References

Abu Dhabi (2016) International renewable energy agency. Innovation outlook: offshore wind. Available from http://www.irena.org/Publications

API RP 17B (2008) Recommended practice for flexible pipe. American Petroleum Institute, 4th ed

Bahaj ABS (2011) Generating electricity from the oceans. Renew Sust Energ Rev 15(7):3399–3416. https://doi.org/10.1016/j.rser.2011.04.032

Bassett K, Carriveau R, Ting SK (2016) Underwater energy storage through application of Archimedes principle. Journal of Energy Storage 8:185–192. https://doi.org/10.1016/j.est.2016.07.005

Boom H, Dekker JN, Elsacker AWV (1987) Dynamic aspects of offshore riser and mooring concepts. J Pet Technol 40(12):1609–1616

Cuamatzi-Melendez R, Castillo-Hernández O, Vázquez-Hernández AO, Vaz MA (2017) Finite element and theoretical analyses of bisymmetric collapses in flexible risers for deepwaters developments. Ocean Eng 140:195–208. https://doi.org/10.1016/j.oceaneng.2017.05.032

DNV, G (2014) Electrifying the future. DNV GL, Høvik

European Commission (2014) Blue Energy. Action needed to deliver on the potential of ocean energy in European seas and oceans by 2020 and beyond

Germa JM, MGH-deep sea storage (2010). Available from http://www.mgh-energy.com/ [accessed 10.03.17]

Ghadimi R (1988) A simple and efficient algorithm for the static and dynamic analysis of flexible marine risers. Comput Struct 29:541~544

Gobat JI (2000) The dynamics of geometrically compliant mooring systems

Government HM (2010) Marine Energy Action Plan 2010: executive summary & recommendations

Hahn H, Hau D, Dick C, Puchta M (2017) Techno-economic assessment of a subsea energy storage technology for power balancing services. Energy 133:121–127. https://doi.org/10.1016/j.energy.2017.05.116

Hill T, Zhang Y, Kolanski T (2006) The future for flexible pipe riser technology in deep water: case study. Offshore Technology Conference, 1–4 May, Houston, Texas, USA. https://doi.org/10.4043/17768-MS

Hoffman D, Ismail N, Nielsen R, Chandwani R (1991) The design of flexible marine risers in deep and shallow water. Offshore Technology Conference, 6–9 May, Houston, Texas. https://doi.org/10.4043/6724-MS

Huang S, Vassalos D (1993) A numerical method for predicting snap loading of marine cables. Appl Ocean Res 15(4):235–242. https://doi.org/10.1016/01411187(93)90012-M

Hydrostor Corp (2015) Hydrostor activates world's first utility-scale underwater compressed air energy storage system. Available form https://hydrostor.ca/press/Hydrostor_Press_Release_-_Nov_18_2015_FINAL.pdf

Institution BS (2006) Petroleum and natural gas industries. Design and operation of subsea production systems. Unbonded flexible pipe systems for subsea and marine applications. Available form https://www.bsbedge.com/productdetails/BSI/BSI30202572/bseniso13628-2

Jain AK (1994) Review of flexible risers and articulated storage systems. Ocean Eng 1994:733–750

Kamman JW, Huston RL (2001) Multibody dynamics modeling of variable length cable systems. Multibody Sys Dyn 5(3):211–221

Komor P, Glassmaire J (2012) Electricity storage and renewables for island power

Kordkheili SAH, Bahai H (2007) Non-linear finite element static analysis of flexible risers with a touch down boundary condition. ASME 2007 International Conference on Offshore Mechanics and Arctic Engineering, 443–447

Lan H, Wen S, Hong YY, Yu DC, Zhang L (2015) Optimal sizing of hybrid PV/diesel/battery in ship power system ☆. Appl Energy 158:26–34

Li B, Decarolis JF (2015) A techno-economic assessment of offshore wind coupled to offshore compressed air energy storage. Appl Energy 155:315–322

Lim SD, Mazzoleni AP, Park JK, Ro PI, Quinlan B (2013) Conceptual design of ocean compressed air energy storage system. Mar Technol Soc J 47(2):1–8

Liu JY, Zhang L (2016) Strategy design of hybrid energy storage system for smoothing wind power fluctuations. Energies 9:990–991

Long YU, Tan J (2005) Model of mooring line and seabed interaction and its nonlinear analysis. Offshore Platform 20(2):20–25

Lshii K, Makino Y, Fuku T, Kagoura T, Yoshizawa M, Wada H (1995) Flexible riser technology for deep water applications. Offshore Technology Conference, 1–4 May, Houston, Texas. https://doi.org/10.4043/7726-MS

Miao H (1998) A time domain computation method for dynamic behavior of mooring system. China Ocean Engineering 12(1):1–10

ORCAFLEX (2017). ORCAFLEX help file and user manual. Available from www.orcina.com

Pham DC, Sridhar N, Qian X, Sobey AJ, Achintha M, Shenoi A (2016) A review on design, manufacture and mechanics of composite risers. Ocean Eng 112:82–96. https://doi.org/10.1016/j.oceaneng.2015.12.004

Pimm AJ, Garvey SD, Jong MD (2014) Design and testing of energy bags for underwater compressed air energy storage. Energy 66(2):496–508. https://doi.org/10.1016/j.energy.2013.12.010

Raman NW, Baddour RE (2003) Three-dimensional dynamics of a flexible marine riser undergoing large elastic deformations. Multibody Sys Dyn 10(4):393–423

Santillan ST (2007). Analysis of the elastica with applications to vibration isolation. Dissertations & Theses–Gradworks

Santillan ST, Virgin LN (2011) Numerical and experimental analysis of the static behavior of highly deformed risers. Ocean Eng 38(13):1397–1402. https://doi.org/10.1016/j.oceaneng.2011.06.009

Serna Á, Yahyaoui I, Normey-Rico JE, Prada CD, Tadeo F (2016) Predictive control for hydrogen production by electrolysis in an offshore platform using renewable energies. Int J Hydrog Energy 42(17):42–12876. https://doi.org/10.1016/j.ijhydene.2016.11.077

Slocum AH, Fennell GE, Dundar G, Hodder BG, Meredith JDC, Sager MA (2013) Ocean renewable energy storage (ORES) system: analysis of an undersea energy storage concept. Proc IEEE 101(4):906–924. https://doi.org/10.1109/JPROC.2013.2242411

Stegman A, Andres AD, Jeffrey H, Johanning L, Bradley S (2017) Exploring marine energy potential in the UK using a whole systems modelling approach. Energies 10(9):1251. https://doi.org/10.3390/en10091251

Tang X, Sun Y, Zhou G, Miao F (2017). Coordinated control of multi-type energy storage for wind power fluctuation suppression. https://doi.org/10.3390/en10081212

The Mid-Atlantic Regional Planning Body (2016). The Mid-Atlantic Regional Ocean Action Plan

Vasel-Be-Hagh AR, Carriveau R, Ting DSK (2015) Structural analysis of an underwater energy storage accumulator. Sustainable Energy Technol Assess 11:165–172. https://doi.org/10.1016/j.seta.2014.11.004

Wang J, Duan M (2015) A nonlinear model for deep water steel lazy-wave riser configuration with ocean current and internal flow. Ocean Eng 94:155–162

Wang ZW, Xiong W, Ting SK, Carriveau R, Wang ZW (2016) Conventional and advanced exergy analyses of an underwater compressed air energy storage system. Appl Energy 180:810–822. https://doi.org/10.1016/j.apenergy.2016.08.014

Wang J, Lu K, Ma L, Wang J, Dooner M, Miao S, Li J, Wang D (2017) Overview of compressed air energy storage and technology development. Energies 10(7):991. https://doi.org/10.3390/en10070991

Xie N, Gao HQ (2000). Two-dimensional time domain dynamic analysis for the general buoy-cable-body system. J Hydrodyn

You T, Su Z, Ruo Z (2008). Advance of study on dynamic characters of mooring systems in deep water. Ocean Eng

Yu ZB, Ning HE, Gao S (2014). Flexible pipe risers system in deepwater oil & gas development. Pipeline Technique & Equipment

Yuan M, Fan J, Miao GP (2010a) Dynamic analysis of a mooring system. Chinese Journal of Hydrodynamics 25(3):285–291

Yuan M, Fan J, Miao GP (2010b) Mooring performance of nonlinear elastic mooring lines. Journal of Shanghai Jiaotong University 44(6):820–827

Zanuttigh B, Angelelli E, Kortenhaus A, Koca K, Krontira Y, Koundouri P (2016) A methodology for multi-criteria design of multi-use offshore platforms for marine renewable energy harvesting. Renew Energy 85:1271–1289. https://doi.org/10.1016/j.renene.2015.07.080

Zhou Z, Benbouzid M, Charpentier JF, Scuiller F, Tang T (2013) A review of energy storage technologies for marine current energy systems. Renew Sust Energ Rev 18(2):390–400. https://doi.org/10.1016/j.rser.2012.10.006

Zhou Q, Wang N, Ran L, Shen H, Lv Q, Wang M (2016) Cause analysis on wind and photovoltaic energy curtailment and prospect research in China. Electric Power 49(9):7–12

Zhu H, Gao Y (2017) Vortex induced vibration response and energy harvesting of a marine riser attached by a free-to-rotate impeller. Energy 134:532–544. https://doi.org/10.1016/j.energy.2017.06.084

Zhu KQ, Li DG, Li W (2002) Lumped-parameter analysis method for time-domain of ocean cable-body systems. Ocean Eng 20(2):100–104

Zhu H, Sun Z, Gao Y (2017) Numerical investigation of vortex-induced vibration of a triple-pipe bundle. Ocean Eng 142:204–216. https://doi.org/10.1016/j.oceaneng.2017.07.019